10ème Congrès Français d'Acoustique

Lyon, 12-16 Avril 2010

Verification of hearing protectors' performance in situ: from experimental to practical approach.

Annelies Bockstael[1], Bart Vinck[2], Dick Botteldooren[1]

[1] Ghent University, INTEC, Sint-Pietersnieuwstraat 41 , 9000 Gent, Belgium annelies.bockstael@ugent.be

[2] Ghent University, ORL, De Pintelaan 185 2P1 , 9000 Gent, Belgium

Research has demonstrated that the implementation of hearing protectors to prevent noise-induced hearing loss merits from individual verification at the workfloor. Therefore, the MIRE (Microphone In Real Ear) technique has been adapted for custom-made earplugs with an inner bore drilled over the plug's total length. So a microphone can be inserted to measure via this test bore the sound pressure level behind the hearing protector. The measurement setup appears to be practically feasible, but a clear discrepancy is expected between the sound pressure level at the microphone and the level of interest at the eardrum. To gain insight into this difference - henceforth called transfer function – research has first been conducted with a HATS (Head And Torso Simulator) equipped with the custom-made earplugs. More concrete, the transfer function between the sound pressure at the HATS 'eardrum' and the MIRE microphone has been measured and numerically simulated with the FDTD approach (Finite-Difference Time-Domain). They appear to be stable and reproducible, moreover their most distinct characteristics can be traced down to the main acoustical features of earplug and ear canal. Further, the influence of an individual's specific geometry of the earplug– ear canal complex on the transfer functions has been addressed by performing measurement and simulations with human subjects similar to the research conducted with the HATS. The concordance between individualized simulations and measurements is very satisfying, but the computational cost of the FDTD technique is too large to be implemented in measurement equipment used to test hearing protectors at the workfloor. Therefore a filter approach has been developed based on the FDTD model. The filter transfer functions show good resemblance with the original measurements and simulations if the length of the test bore and of the residual part of the ear canal are taken into account.

1 Introduction

The European Noise Directive [1] on exposure limit values stipulates that a worker's effective exposure must take account of the attenuation provided by his hearing protectors. In this regard, protectors merit individual field attenuation measurements [2] given the well-known discrepancy between the attenuation measured in laboratory conditions and the real protection offered to an individual user [3].

Therefore different measurements procedures have been developed to assess hearing protectors in situ [4]. Among them, a Microphone In Real Ear (MIRE) based approach appears to provide the most effective means to conduct field measurements, yielding to the best trade-off between speed, accuracy, repeatability and correspondence with actual practice [5].

Thus, a custom-made earplug has been designed with an inner bore that allows the insertion of a miniature microphone registering sound pressure levels inside the ear canal behind the hearing protector [6]. In practice, this MIRE measurement microphone is mounted in a probe that also contains a reference microphone measuring the sound pressure outside the ear canal (see Figure 1). One critical issue at this is the manifest difference between the sound pressure level registered at the MIRE measurement microphone and the level of interest

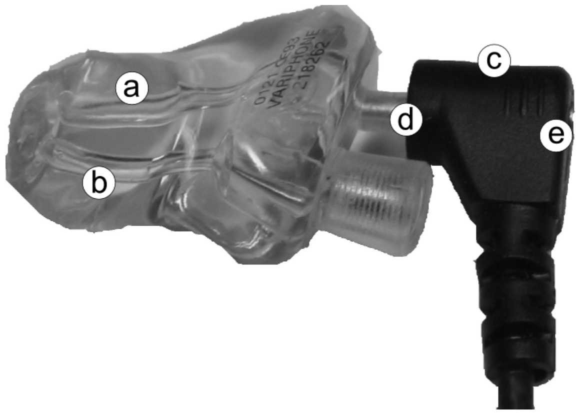

FIGURE 1 – Earplug with two inner bores ; one to adjust the attenuation (b) and the other test bore (a) for insertion of the MIRE probe (c) with measurement (d) and reference (e) microphone. The measurement microphone measures the sound level in the ear canal behind the hearing protector whereas the reference microphone registers the incoming sound level.

at the eardrum.

To gain insight into this difference, henceforth called transfer function, measurements have been performed with a Head And Torso Simulator (HATS) and with human subjects. Additionally, these transfer functions are modeled with Finite-Difference Time-Domain (FDTD) simulations of an ear canal occluded by an earplug [7]. This approach is quite accurate for both the HATS and human ears if the most striking geometrical features of a particular ear and hearing protector are included in an individualized model [8]. Unfortunately, the FDTD simulations require a lot of computer time and can therefore not be incorporated in field measurement equipment. To overcome this problem, a set of digital filters has been computed to allow the deduction of the sound pressure level at the eardrum starting from measurements by the MIRE measurement microphone.

2 Material and methods

2.1 Measurements of the transfer function

For both the HATS and the nineteen human subjects, custom-made acrylic earplugs are manufactured, similar to the hearing protector depicted in Figure 1. All measurements take place in an anechoic room to prevent disturbances from background noise or reverberation.

The MIRE measurements are performed with the probe (see also Figure 1) containing a measurement and a reference microphone, i.c. Knowles low noise FG-3652 microphones. The HATS used in this project is a Brüel & KjærHATS type 4128 C. That device is equipped with an ear simulator which makes it possible to register the sound pressure level where anatomically the eardrum is found. This way, the sound pressure levels at the MIRE measurement microphone and at the HATS's eardrum can be measured simultaneously in response to low pass filtered pink noise with a cutoff frequency of 12.8 kHz. Thus the transfer function H_{me} can be calculated directly by applying the following equation

$$H_{me} = \sqrt{\frac{G_{me}(k)}{G_{mm}(k)} \cdot \frac{G_{ee}(k)}{G^{*}_{me}(k)}}. \tag{1}$$

In equation 1 H_{me} is the frequency response between the MIRE measurement microphone $_m$ and the eardrum $_e$, $G_{mm}(k)$ and $G_{ee}(k)$ are the respective autospectra, $G_{me}(k)$ is the cross-spectrum and $G^{*}_{me}(k)$ its complex conjugate.

Since the captured transfer functions should be absolutely independent of the test signal, the test space and the microphones, two reference free-field microphones are incorporated. All calibration steps are described in detail in previous work [7].

For the human subjects, a similar approach is followed by inserting an extra GN ReSound Aurical microphone in the outer ear canal. This device is designed to measure the sound pressure level at the eardrum and consists of a flexible silicone tube (outer diameter 0.85 mm) connected to an ear piece with microphone. The general approach is very similar to the measurements with the HATS and all details have been described previously [8]. One important remark is that the presence of the flexible silicone tube will not alter sound propagation in the outer ear canal an sich [9] but it does affect the attenuation of the earplug. This seems not critical since previous analysis have pointed out that changing the earplug's attenuation does not influence the difference in sound pressure level between the MIRE measurement microphone and the eardrum [7].

2.2 Simulations of the transfer functions

The sound pressure distribution in an ear canal occluded by an earplug is numerically simulated using the Finite-Difference Time-Domain (FDTD) technique. A key factor of this approach is that both pressure p and particle velocity $\mathbf{u}$ are discretised in Cartesian grids. These grids are staggered by shifting the grid for discretising $\mathbf{u}_\alpha$ over half of a grid step, $\frac{d\alpha}{2}$, in direction α with respect to the grid chosen for discretising p. In time, staggering is obtained by calculating p at $t = ldt$ and $\mathbf{u}$ at $t = (l + \frac{1}{2})dt$. The resulting equations

$$u_\alpha^{l+\frac{1}{2}}(\alpha+\frac{1}{2}) = u_\alpha^{l-\frac{1}{2}}(\alpha+\frac{1}{2}) - \frac{dt}{\rho_0 d\alpha}\{p^l(\alpha+1)-p^l\} \tag{2}$$

$$p^{l+1} = p^l - \sum_{\beta=x,y,z} \frac{\rho_0 c^2 dt}{d\beta}\{u_\beta^{l+\frac{1}{2}}(\beta+\frac{1}{2}) - u_\beta^{l+\frac{1}{2}}(\beta-\frac{1}{2})\} \tag{3}$$

with c the speed of sound and ρ_0 the density of air, allow to step in time replacing old values by newly calculated ones without much memory overhead. The brief notation $(\alpha + q)$ is used to indicate that the value is taken at a point shifted by q spatial steps $d\alpha$ in the α-direction with respect to the reference location referred to by indices (i, j, k). The first equation is repeated for $\alpha = x, y,$ and z where x and y are defined along the cross-section of the ear canal and z represents the longitudinal axis. In the numerical model of the occluded ear, two points of interest are defined where the sound pressure is registered, namely in front of the eardrum and at the end of the test bore where in reality the MIRE measurement microphone is placed.

The acoustically important features of the hearing protector's material [10], the ear canal's wall [11] and the middle and inner ear [12] are introduced in the model by boundary impedance of the form

$$Z = j\omega Z_1 + Z_0 + \frac{Z_{-1}}{j\omega} \tag{4}$$

which can be easily implemented in FDTD [13].

Apart from these general considerations, individual differences in ear canal and hearing protector might also mark the transfer function. Therefore, the most striking geometrical features that are thought to influence sound propagation are accurately measured for each test subject and the HATS and included in the simulations with a 0.35 mm gridcell size.

2.3 Approximating transfer functions by filtering

For the complex frequency response of the FDTD simulated transfer function the corresponding continuous-time transfer function is found using *invfreqs* (MATLAB) because this algorithm guarantees stability of the resulting linear system. The corresponding complex frequency response $H(s)$ can be written as

$$H(s) = \frac{B(s)}{A(s)} = \frac{b_{(1)}s^n + b_{(2)}s^{n-1} + \ldots + b_{(n+1)}}{a_{(1)}s^n + a_{(2)}s^{n-1} + \ldots + a_{(n+1)}} \quad (5)$$

with $s = i2\pi f$, f representing the frequency.

The frequency range of interest is set between 0 Hz and 8000 Hz analogous to the frequencies tested with pure-tone audiometry [14]. The filter coefficients are deliberately determined in the s-domain instead of the z-domain. In that way, the resulting filter can be digitalized afterwards with a sampling frequency adapted to the sampling frequency of the measurement system used in practice. When choosing the order of 6 for both $B(s)$ and $A(s)$, the frequency response of the analogue filter $H(s)$ is almost identical to the FDTD simulated transfer function.

After the filtering, linear regression is carried out to predict the position of each pole and zero of the filter, i.e. the roots of respectively $A(s)$ and $B(s)$. More specifically, the aim of the multiple linear regression is to find for each pole and zero a formal relationship with one or more geometrical variables. In this way, the values of the geometrical parameters for a specific individual can serve as input to calculate the corresponding poles and zeros. The resulting individualized filter can be used in the measurement equipment to predict the sound pressure at the eardrum from the response of the MIRE measurement microphone.

The real poles and zeros can serve directly as dependent variables. For the complex ones, the real and the imaginary part are fitted separately. Because all coefficient are real, the complex conjugate of each complex pole or zero is also a pole or zero of the filter under study. In that case, only the real and imaginary part of the pole/zero with a positive imaginary part are considered for linear regression. The corresponding complex conjugate can then be easily deduced from the resulting formulas.

Possible independent variables are selected according to the individualized geometrical input variables for the FDTD simulations. Care is taken that none of the selected variables can be written as a linear combination of the others.

Prior to the regression analysis, the correlation is calculated between each dependent variable and all candidate independent variables by drawing up a Pearson correlation table. Based on this table, a manual step-forward regression procedure is followed. This means that one independent variable is added at the time, starting with the variable that shows the strongest linear correlation with the dependent variable. The procedure is repeated until the adjusted R^2 equals or exceeds 0.80 and the residuals of the final model are normally distributed [15]. This procedure results in an expression to

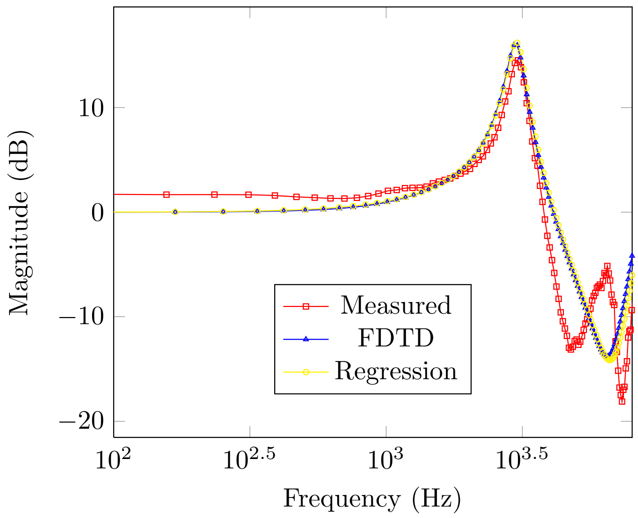

Figure 2 – Comparison of the transfer functions of one particular human ear as obtained by measurements ('Measured'), FDTD simulations ('FDTD') and multiple linear regression ('Regression').

estimate the expected value of the dependent variable $\hat{y}$ based on one or more independent variables x

$$\hat{y} = d_0 + d_1 x_1 + \ldots + d_n x_n. \quad (6)$$

3 Results

3.1 Measured transfer functions

In Figure 2 an example of a measured transfer function is shown. All transfer functions appear to have the same global form with a distinct maximum between 2500 Hz and 3500 Hz and multiple minima above 4500 Hz. Often the most distinct minimum is seen between 4500 Hz and 6500 Hz. Combining the results from measurements with the HATS and human subjects leads to the conclusion that the first maximum is most probably caused by resonance in the test bore, picked up by the MIRE measurement microphone and absent at the eardrum. Additionally, the most distinct minimum is most likely due to resonances in the residual part of the ear canal behind the hearing protector, present at the eardrum but not at the MIRE measurement microphone.

Despite the common global shape, the intersubject variability appears to be substantial with respect to the exact frequency and amplitude of the extrema. This is little surprising given the relationship between the appearance of the transfer function and the particular structures of one's ear canal and hearing protector.

3.2 Simulated transfer functions

Figure 2 also reveals that the simulated transfer function is very similar to that measured. The frequency dependence at the lower frequencies is very well predicted. As for the amplitude, all the numerical simulations have a constant amplitude of 0 dB whereas most measurements reach constant values between 0 dB and 5 dB. It is experimentally verified that bending the probe tube can indeed lower the response of the Aurical microphone up to 5 dB in the lower frequency range. Flexures of the tube could not be avoided due to the relatively difficult positioning of the tube in an ear canal occluded by an earplug, but the influence of the bends can be clearly identified and hence the difference between the simulated and measured transfer function below 1500 Hz is not considered critical [8]. Further, the frequency and amplitude of the first maximum are very well approached by the model. Slight differences in the frequency of the most distinct minimum between 4500 Hz en 6500 Hz are not of great interest because they are among other things influenced by the exact position of the earplug which might vary from one measurement to another [8]. For frequencies above 6500 Hz, the numerical model and the measurements still show resembling frequency dependence but the resemblance is decreased compared to the frequency region below 6500 Hz [7].

3.3 Filter approximation to transfer functions

Performing linear regression points out that two geometrical parameters suffice to predict the poles and zeros with reasonable accuracy, namely the length of test bore (see Figure 1) and the length of the residual part of the ear canal between hearing protector and eardrum. The regression models are quite straight forward for most poles and zeros with adjusted R^2 values easily exceeding 0.80. For the real part of the fifth pole and the fifth zero, the adjusted R^2 only reaches values of respectively 0.74 and 0.75. Since adding more variables does not substantially increases this value and since the residuals of the models are normally distributed, the most simple models with the highest adjusted R^2 is chosen.

For the first and second zero, the regression analysis becomes much more complicated because most ears have real first and second zeros, but a distinct minority has complex ones. The complex zeros tend to be associated with longer ear canals in combination with a shorter test bore. Despite this association, it is not possible to accurately predict whether a certain ear will deviate from the majority by having a complex first and second zero. Given the limited number of ears resulting in complex first and second zeros, only the real ones are used for linear regression. Naturally, this implies that the regression model might be less accurate for longer ear canals.

However, for the ears that have more average dimensional parameters, the filter with poles and zeros coming from the regression models resembles the original transfer functions quite well (see Figure 2). This implies that for those ears the transfer function can be predicted if only the length of the test bore and the residual part of the ear canal are known.

4 Discussion

Previous research has demonstrated that the MIRE method is a suitable way to measure the performance of hearing protectors in situ. [5]. Further, the transfer functions predicted from the FDTD model are in good agreement with the measured transfer functions, especially in the frequency region below 6000 Hz [7]. Above this frequency, the numerical simulations still follow the trend of the measurements, but differences in amplitude increase.

It is indeed possible that the numerical model is less accurate for higher frequencies because the bended character of the ear canal [16] is not included in this model, nor is the more complex vibration pattern of the eardrum at higher frequencies [17]. Besides these considerations, the question arises whether it is actually possible to approach the true transfer function correctly in this higher frequency region. Even very small variations in the position of the earplug may distinctly alter the frequency response of the ear canal's residual part, changing the appearance of the transfer function for frequencies above 4500 Hz. Even in general, the variability of measured attenuation seems to increase with increasing frequency [5].

This report also shows that the simulated transfer function can be approximated with linear regression, only the length of the ear canal and the test bore needs to be known. The total length of the ear canal can easily be measured by sliding a silicone tube into the ear canal, for example at the time that the ear impression for the custom-made earplug is taken. The length of the earplug itself and of its inner bore can be determined during the manufacturing process.

With these parameters, it takes negligible computer time to actually evaluate the individualized transfer function. Therefore, there is no real need to calculate the transfer function beforehand - although it is possible - but instead the computation can be carried out when the MIRE measurement is performed.

Finally, it appears that the model performs well for a considerable range of possible values for the independent parameters. However, for rather rare combinations of a shorter test bore and a longer ear canal, the prediction is inaccurate. In this regard, further research seems advisable.

Références

[1] "Directive 2003-10-EC on the minimum health and safety requirements regarding the exposure of workers to the risks arising from physical agents (noise)". European Parliament and Council, Brussels (2003).

[2] Berger, E. H., Franks, J. R., Lindgren, F. "International review of field studies of hearing protection attenuation". pages 361–377. Thieme Medical Pub, New York (1996).

[3] Franks, J. "Comparison of the regulatory noise reduction rating (NRR) and the required ANSI S3.19 test method with real world outcomes and results from testing with the new ANSI S12.6B method". In "Workshop on hearing protector devices", United States Environmental Protection Agency, Washington DC (2003).

[4] Casali, J. G., Mauney, D. W., Alton, B. J. "Physical vs. psychophysical measurements of hearing protection attenuation - a.k.a. MIRE vs. REAT". *Sound Vib.* pages 20–27 (1995).

[5] Berger, E. H., Voix, J., Kieper, R. W. "Methods of developing and validating a field-mire approach for measuring hearing protector attenuation". In "Spectrum", volume 24 of *Suppl 1.* 32nd Annual Conference of the National Hearing Conservation Association, Savannah GA (2007).

[6] Voix, J. *Mise au point d'un bouchon d'oreille 'intelligent' (Development of a 'smart' earplug).* Ph.D. thesis, Ecole de Technologie Supérieure Université du Québec (2006).

[7] Bockstael, A., et al. "Verifying the attenuation of earplugs in situ : method validation using artificial head and numerical simulations". *J. Acoust. Soc. Am.* 124 (2), 973–981 (2008).

[8] Bockstael, A., et al. "Verifying the attenuation of earplugs in situ : method validation on human subjects including individualized numerical simulations". *J. Acoust. Soc. Am.* 125 (3), 1479–1489 (2009).

[9] Hellstrom, P.-A., Axelsson, A. "Miniature microphone probe tube measurements in the external auditory canal". *J. Acoust. Soc. Am.* 93 (2), 907–919 (1993).

[10] Hillström, L., Mossberg, M., Lundberg, B. "Identification of complex modulus from measured strains on an axially impacted bar using least squares". *J. Sound Vib.* 230 (3), 689–707 (2000).

[11] Wit, H. P., Damme, K. J., Van Spoor, C. W. *Fysica voor de fysiotherapeut (Physics for the physiotherapist).* Bunge, Utrecht (1987).

[12] Kringlebotn, M. "Network model of the human middle ear". *Scandinavian Audiology* 17, 75–85 (1988).

[13] Botteldooren, D. "Finite-difference time-domain simulation of low-frequency room acoustic problems". *J. Acoust. Soc. Am.* 98, 3302–3308 (1995).

[14] International Standard Organisation. (1989).

[15] Kutner, M. H., Nachtscheim, C. J., Neter, J., Li, W. *Applied linear statistical models.* McGraw-Hill, New York, 5th edition (2004).

[16] Koike, T., Wada, H., Kobayashi, T. "Modeling of the human middle ear using the finite-element method". *J. Acoust. Soc. Am.* 111 (3), 1306–1317 (2002).

[17] Tonndorf, J., Khanna, S. M. "Tympanic-membrane vibrations in human cadaver ears studied by time-averaged holography". *J. Acoust. Soc. Am.* 52 (4B), 1221–1233 (1972).